http://doc.rero.ch

Selective lesion of the hippocampus increases the differentiation of immature neurons in the monkey amygdala

Loïc J. Chareyron[a], David G. Amaral[b,c], and Pierre Lavenex[a,d,1]

[a]Laboratory of Brain and Cognitive Development, Department of Medicine, University of Fribourg, 1700 Fribourg, Switzerland; [b]Department of Psychiatry and Behavioral Sciences, MIND Institute, University of California, Davis, CA 95616; [c]California National Primate Research Center, University of California, Davis, CA 95616; and [d]Laboratory for Experimental Research on Behavior, Institute of Psychology, University of Lausanne, 1015 Lausanne, Switzerland

A large population of immature neurons is present in the ventromedial portion of the adult primate amygdala, a region that receives substantial direct projections from the hippocampal formation. Here, we show the effects of neonatal ($n = 8$) and adult ($n = 6$) hippocampal lesions on the populations of mature and immature neurons in the paralaminar, lateral, and basal nuclei of the adult monkey amygdala. Compared with unoperated controls ($n = 7$), the number of mature neurons was about 70% higher in the paralaminar nucleus of neonate- and adult-lesioned monkeys, and 40% higher in the lateral and basal nuclei of neonate-lesioned monkeys. The number of immature neurons in the paralaminar nucleus was 40% higher in neonate-lesioned monkeys and 30% lower in adult-lesioned monkeys. Similar changes in neuron numbers were also found in two monkeys with nonexperimental, selective, bilateral hippocampal damage. These changes in neuron numbers following hippocampal lesions appear to reflect the differentiation of immature neurons present in the paralaminar nucleus. After adult lesions, the differentiation of immature neurons was essentially restricted to the paralaminar nucleus and was associated with a decrease in the population of immature neurons. In contrast, after neonatal lesions, the differentiation of immature neurons involved the paralaminar, lateral, and basal nuclei. It was associated with an increase in the population of immature neurons in the paralaminar nucleus. Such lesion-induced neuronal plasticity sheds new light on potential mechanisms that may facilitate functional recovery following focal brain injury.

immature neuron | migration | subventricular zone | plasticity | neurodevelopmental disorders

Previous studies have shown the existence of cells expressing markers typically associated with immature neurons in various regions of the adult mammalian brain (1–5), which suggested a strong potential for neuronal plasticity following focal brain injury in adult individuals (6–9). One such brain region that contains a large population of immature neurons at birth is situated along the temporal horn of the lateral ventricle and includes the paralaminar nucleus of the amygdala in monkeys (3, 10, 11) and humans (5). These immature neurons are positive for Bcl2, class III β-tubulin, doublecortin (DCX), and polysialylated neural cell adhesion molecule (PSA-NCAM) (3, 12–15). In monkeys, the population of immature neurons present in the paralaminar nucleus at birth decreases after 1 y of age (10). At the same time, the number of mature neurons increases, thus suggesting that neuronal differentiation occurs in the amygdala over a prolonged course of postnatal development. However, a large population of immature-looking neurons remains into adulthood (10). Additionally, although a number of cellular mechanisms involved in the regulation of postnatal neurogenesis in neurogenic brain regions have been identified (16), the specific factors that may induce the differentiation of immature neurons in nonneurogenic regions are largely unknown. Among general factors that impact cell proliferation in neurogenic regions (17), focal brain lesions may also influence the differentiation of immature neurons in the postnatal monkey amygdala.

Because the amygdala is an important target of sensory information processed by the hippocampus (18, 19), it is plausible that hippocampal lesions may induce changes in neuronal structure and function in the primate amygdala. In monkeys, cells located mostly along the border of CA1 and the subiculum project to the paralaminar nucleus and the ventral part of the basal nucleus (20, 21). Interestingly, these projections overlap with the population of immature amygdala neurons (3, 13). Hippocampal function, or lack thereof, may thus exert a modulatory influence on the postnatal maturation and plasticity of amygdala neurons. Here, we report the effects of neonatal and adult hippocampal lesions on the populations of mature and immature neurons in the paralaminar, lateral, and basal nuclei of the adult monkey amygdala. We show that, compared with unoperated controls, selective hippocampal lesion increases the differentiation of immature neurons in the monkey amygdala.

Experimental Procedures

Twenty-three macaque monkeys (*Macaca mulatta*) were used for this study. Monkeys were naturally born from multiparous mothers and raised at the California National Primate Research Center. Bilateral hippocampal lesions were performed following the same protocol for both neonatal (12–16 d after birth) and adult (at 6.7–9.7 y of age) lesion groups (Fig. 1). Detailed procedures are described in refs. 22 and 23. Lesion extent is described in *SI Experimental Procedures*. Experimental procedures were approved by the Institutional Animal Care and Use Committee of the University of California, Davis, and were conducted in accordance with the National Institutes of Health guidelines for the use of animals in research. To reduce the number of animals used for research, all monkeys had been involved in other studies before being recruited for this study.

Significance

A large population of immature neurons has been reported in the ventromedial portion of the adult primate amygdala. Here, we show that selective hippocampal lesions lead to an increase in mature neuron numbers in the monkey amygdala. After adult lesions, the differentiation of immature neurons was essentially restricted to the paralaminar nucleus and was associated with a decrease in the population of immature neurons in the paralaminar nucleus. In contrast, after neonatal lesions, the differentiation of immature neurons involved the paralaminar, lateral, and basal nuclei, and was associated with an increase in the population of immature neurons in the paralaminar nucleus. This is unique evidence of lesion-induced alterations in the number of neurons in the nonhuman primate amygdala.

Author contributions: L.J.C., D.G.A., and P.L. designed research; L.J.C., D.G.A., and P.L. performed research; L.J.C. and P.L. analyzed data; and L.J.C., D.G.A., and P.L. wrote the paper.

The authors declare no conflict of interest.

[1]To whom correspondence should be addressed. Email: pierre.lavenex@unil.ch.

This article contains supporting

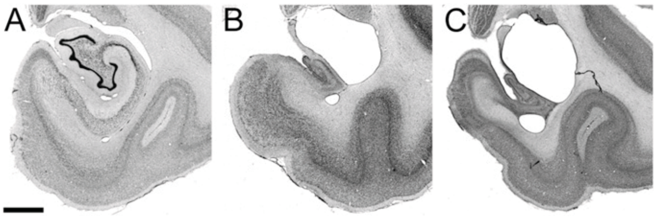

Fig. 1. Lesion evaluation. Nissl-stained sections of the monkey medial temporal lobe at midrostrocaudal level of the hippocampus [Bregma −15.3 (43)]. (*A*) Adult, unoperated control monkey. (*B*) Adult monkey with neonatal hippocampal lesion. (*C*) Adult monkey with adult hippocampal lesion. (Scale bar for all three panels, 2 mm.)

Unoperated Control Monkeys (n = 7). Four adult monkeys (5.3–9.4 y) were used in quantitative studies of the monkey hippocampal formation (24, 25) and amygdala (10, 26). Four monkeys (9.2–9.5 y) were added to serve as unoperated controls for the current study. One of these monkeys [nonexperimental hippocampal lesion (NEHL)1; 9.4 y] had a nonexperimental, selective lesion of the hippocampus and is thus considered separately in this study (*SI Experimental Procedures* and Fig. S1).

Neonatal Hippocampal-Lesioned Monkeys (n = 8). These eight animals were part of a longitudinal study of the effects of neonatal damage to the amygdala or hippocampus on the development of social behavior (27–29). They were 9.1–9.4 y of age at the time their brains were collected.

Adult Hippocampal-Lesioned Monkeys (n = 6). These six animals were used in a study of the role of the hippocampus in spatial learning in adult macaque monkeys (23). One additional monkey (NEHL2; 12.6 y) originally assigned to the study's control group had a nonexperimental, selective lesion of the hippocampus (23) and is thus considered separately in this study (*SI Experimental Procedures*).

Histological Procedures. Brain acquisition and Nissl staining of brain sections followed our standard laboratory protocol (30). In addition, we used fluorescence immunohistochemistry and three cell-specific markers, NeuN, Bcl2, and DCX to characterize the phenotypes of cells in the ventromedial amygdala. NeuN is a well-established neuron-specific marker (31). Bcl2 is an antiapoptotic protein, which influences the rate of neuronal differentiation in young neurons and is expressed in populations of immature neurons (1). DCX is a well-defined marker of immature neurons (32, 33). We used Bcl2 biotin-immunohistochemistry to label immature neurons and obtain a second estimate of immature neuron numbers. See also *SI Experimental Procedures*.

Data Acquisition. We used design-based stereological techniques (34) on Nissl-stained sections to estimate the numbers of mature and immature neurons in the paralaminar, lateral, and basal nuclei of the amygdala, as well as the volume of the nuclei and the number of Bcl2-labeled immature neurons in the paralaminar nucleus (Tables S1 and S2).

Statistical Analyses. We performed ANOVAs with the time of the lesion as a factor on the volume of amygdala nuclei, the number of mature neurons, immature neurons, Bcl2$^+$ cells, and neuronal soma size, because these data were normally distributed. Post hoc analyses were performed with the Fisher least-significant difference test when the ANOVA F ratio was significant and thus controlling for type I error rate (35).

Results

Amygdala Nuclei Volume. The volume of the paralaminar nucleus differed between groups (Fig. S2*A*) [$F_{(2,\ 18)} = 15.594$, $P < 0.001$]. Compared with controls, the paralaminar nucleus was, respectively, 26% and 27% larger in neonate- and adult-lesioned monkeys (both $P < 0.001$). Analyses of the rostrocaudal profile of the paralaminar nucleus revealed that in neonate- and adult-lesioned monkeys, the volumetric increase was most substantial caudally in the nucleus (Fig. S2*B*). There were no differences in the volume of the lateral nucleus between experimental groups (Fig. S2*C*) [$F_{(2,\ 18)} = 0.605$, $P = 0.557$]. There were no differences in the volume of the basal nucleus between experimental groups (Fig. S2*E*) [$F_{(2,\ 18)} = 0.891$, $P = 0.428$].

Mature Neuron Numbers.

Paralaminar nucleus. Compared with controls, the number of mature neurons in the paralaminar nucleus was 72% higher in neonate-lesioned and 65% higher in adult-lesioned monkeys (Fig. 2*A*) [$F_{(2,\ 18)} = 87.520$, $P < 0.001$; Fisher least-significant difference: both $P < 0.001$]. In neonate- and adult-lesioned monkeys, the increase in mature neuron number was distributed along the entire rostrocaudal extent of the paralaminar nucleus (Fig. 2*B*). Neuronal density suggested that the increase in mature neuron number in the paralaminar nucleus was distributed along the mediolateral axis in both neonate- and adult-lesioned monkeys (Fig. 2*C*).

Lateral nucleus. The number of mature neurons in the lateral nucleus was 44% higher in neonate-lesioned monkeys than in controls, and 33% higher in neonate-lesioned monkeys than in adult-lesioned monkeys (Fig. 2*D*) [$F_{(2,\ 18)} = 17.819$, $P < 0.001$; both $P < 0.001$]. Mature neuron number in the lateral nucleus did not differ between adult-lesioned and control monkeys ($P = 0.340$). In neonate-lesioned monkeys, the increase in mature neuron number was distributed along the entire rostrocaudal extent of the lateral nucleus (Fig. 2*E*). In adult-lesioned monkeys, a nonsignificant increase in mature neurons appeared restricted to the rostral part of the lateral nucleus (Fig. 2*E*). Neuronal density suggested that the increase in mature neuron number was distributed throughout the dorsoventral and mediolateral extents of the lateral nucleus in neonate-lesioned monkeys, whereas a nonsignificant increase appeared to be limited to the ventrolateral border of the nucleus in adult-lesioned monkeys (Fig. 2*F*).

Basal nucleus. In the basal nucleus, the number of mature neurons was 35% higher in neonate-lesioned monkeys than in controls, and 45% higher in neonate-lesioned than in adult-lesioned monkeys (Fig. 2*G*) [$F_{(2,\ 18)} = 8.202$, $P = 0.003$; both $P < 0.01$]. The number of mature neurons in the basal nucleus did not differ between adult-lesioned and control monkeys ($P = 0.585$). In neonate-lesioned monkeys, the increase in mature neuron number was distributed along the entire rostrocaudal extent of the basal nucleus (Fig. 2*H*). Neuronal density suggested that, in neonate-lesioned monkeys, the increase in mature neuron number was distributed throughout the dorsoventral and mediolateral extents of the nucleus (Fig. 2*I*).

Immature Neuron Numbers in the Paralaminar Nucleus. The number of immature neurons in the paralaminar nucleus, estimated from Nissl-stained sections, differed between groups (Fig. 3*A*) [$F_{(2,\ 18)} = 24.660$, $P < 0.001$]. The number of immature neurons was 38% higher in neonate-lesioned than in control monkeys ($P < 0.001$) and 88% higher in neonate-lesioned than in adult-lesioned monkeys ($P < 0.001$). The number of immature neurons in the paralaminar nucleus was 27% lower in adult-lesioned monkeys than in controls ($P = 0.012$). In neonate-lesioned monkeys, the increase in immature neuron number appeared to be restricted to the caudal end of the paralaminar nucleus (Fig. 3*B*). In adult-lesioned monkeys, the decrease of immature neurons was distributed along the rostrocaudal extent of the nucleus (Fig. 3*B*).

To confirm the estimates of the number of immature neurons derived from Nissl-stained preparations, we performed a stereological analysis of the number of Bcl2$^+$ cells in the paralaminar nucleus (Fig. 3*D*). The estimates of the number of immature neurons in Nissl-stained sections and the number of Bcl2$^+$ cells were highly correlated (Pearson's correlation, $r = 0.846$, $P < 0.001$). The number of Bcl2$^+$ cells in the paralaminar nucleus differed between groups (Fig. 3*E*) [$F_{(2,\ 18)} = 12.443$, $P < 0.001$]. The number of Bcl2$^+$ cells was 29% higher in neonate-lesioned monkeys than in controls ($P = 0.014$) and 74% higher in neonate-lesioned than in adult-lesioned monkeys ($P < 0.001$). The number of Bcl2$^+$ cells in the paralaminar nucleus was 26% lower in adult-lesioned monkeys than in controls ($P = 0.035$).

Ninety-seven percent of Bcl2$^+$ cells present in the ventromedial amygdala were NeuN$^+$ (Bcl2$^+$/NeuN$^+$) (Fig. 4) and 93% of these Bcl2$^+$/NeuN$^+$ were also DCX$^+$ (Bcl2$^+$/NeuN$^+$/DCX$^+$),

http://doc.rero.ch

http://doc.rero.ch

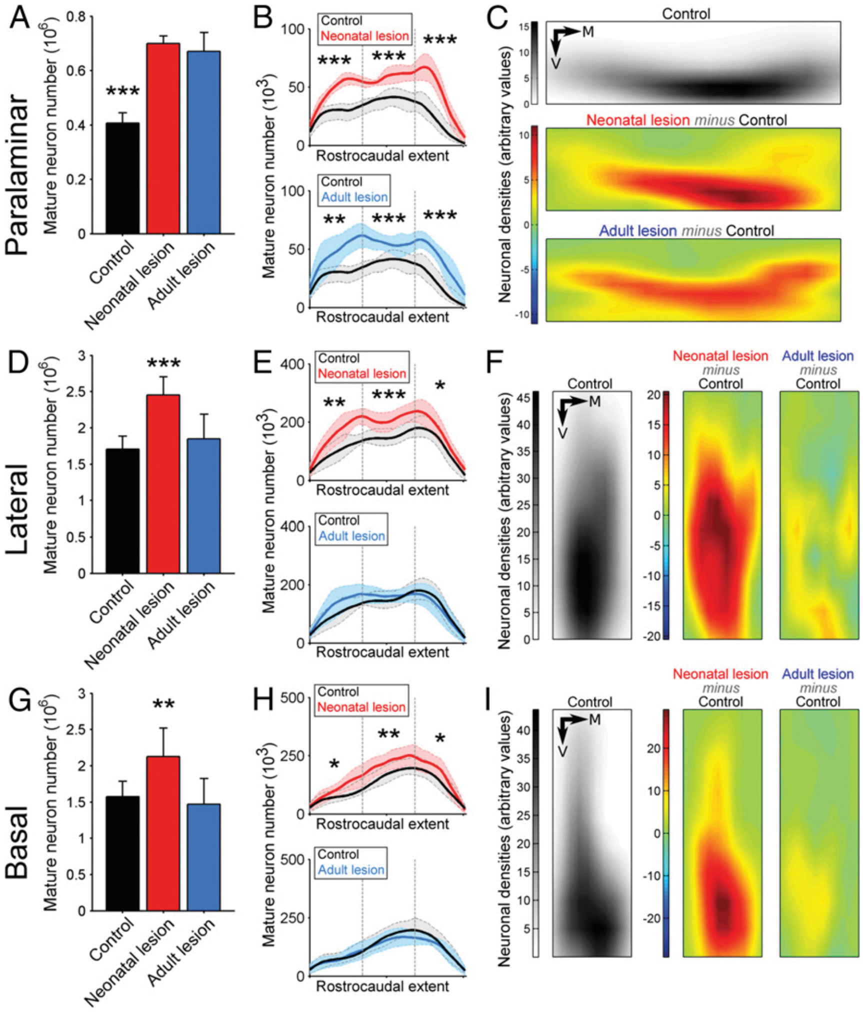

Fig. 2. Mature neurons. Numbers and distributions of mature neurons in the amygdala nuclei of unoperated control (black), neonatal hippocampal-lesioned (red), and adult hippocampal-lesioned (blue) monkeys. (Average ± SD; *$P < 0.05$; **$P < 0.01$; ***$P < 0.001$) (Table S2). (*A–C*) Paralaminar nucleus. (*D–F*) Lateral nucleus. (*G–I*) Basal nucleus. (*A*, *D*, and *G*) Mature neuron numbers. (*B*, *E*, and *H*) Rostrocaudal distributions of mature neurons in the different groups (left = rostral, right = caudal; average ± SD). (*C*, *F*, and *I*) Dorsoventral and mediolateral distributions of mature neurons in the different groups. (*Top*/*Left*) Neuron distribution in control monkeys. (*Middle*) Difference between the cell-density map obtained in neonate-lesioned and control monkeys. (*Bottom*/*Right*) Difference between the cell-density map obtained in adult-lesioned and control monkeys. The strength of the difference is mapped according to an arbitrary color scale (M, medial; V, ventral). Cell-density maps were derived from stereological analysis data. For each monkey, all coronal slices analyzed for each nucleus were aligned along the same axis, centered, stacked, and then summed. We then normalized the *x* and *y* dimensions of the obtained maps (i.e., the height and width of the nuclei) to produce an average map for each experimental group. Thus, density maps do not reflect and do not take into account potential differences in the size of the nuclei. See also Fig. S3.

thus confirming that these cells were immature neurons. See also Figs. S6 and S7. We did not find any difference in the proportion of labeled cell types between control, neonate-lesioned, or adult-lesioned monkeys.

In the paralaminar nucleus, the sum of mature and immature neuron numbers differed between groups (Fig. S5) [$F_{(2, 18)} = 41.193$, $P < 0.001$]. The total number of neurons was 53% larger in neonate-lesioned monkeys than in controls ($P < 0.001$), 34% larger in neonate-lesioned than in adult-lesioned monkeys ($P < 0.001$) and 14% larger in adult-lesioned monkeys than in controls ($P = 0.042$). In neonate-lesioned monkeys, the increase in the total number of neurons was distributed along the entire rostrocaudal extent of the paralaminar nucleus (Fig. S5*B*).

Volume of Mature Neurons.

Paralaminar nucleus. The average soma volume of mature neurons differed between groups in the paralaminar nucleus (Fig. 5*A*) [$F_{(2, 18)} = 11.409$, $P < 0.001$]. It was 15% smaller in neonate-lesioned monkeys than in controls ($P < 0.001$), and 13% smaller in adult-lesioned monkeys than in controls ($P = 0.001$). It did not differ between neonate- and adult-lesioned monkeys ($P = 0.730$). The number of neurons smaller than the controls' median neuron size differed between groups (Fig. 5*B*) [$F_{(2, 18)} = 39.493$, $P < 0.001$]. There were more small mature neurons in neonate- and adult-lesioned monkeys than in controls (both $P < 0.001$). The number of small mature neurons did not differ between neonate- and adult-lesioned monkeys ($P = 0.251$). The number of neurons larger than the controls' median neuron size also differed between groups (Fig. 5*B*) [$F_{(2, 18)} = 4.185$, $P = 0.032$]. There were more large mature neurons in neonate- and adult-lesioned monkeys than in controls ($P = 0.025$, $P = 0.020$). The number of large mature neurons did not differ between neonate- and adult-lesioned monkeys ($P = 0.777$).

Lateral nucleus. There was no difference in the average volume of mature neuron somas between groups in the lateral nucleus (Fig. 5*C*) [$F_{(2, 18)} = 0.083$, $P = 0.920$]. However, the number of neurons smaller than the controls' median neuron size differed between groups (Fig. 5*D*) [$F_{(2, 18)} = 7.354$, $P = 0.005$]. There were more

http://doc.rero.ch

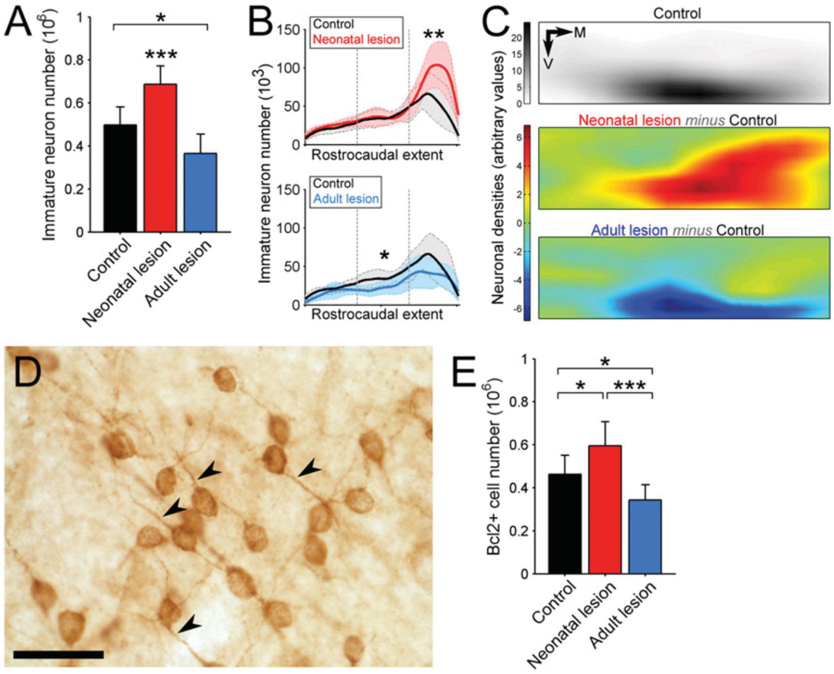

Fig. 3. Immature neurons. Numbers and distributions of immature neurons in the paralaminar nucleus of unoperated control (black), neonatal hippocampal-lesioned (red), and adult hippocampal-lesioned (blue) monkeys. (Average ± SD; $^{*}P < 0.05$; $^{**}P < 0.01$; $^{***}P < 0.001$) (Table S2). (*A*) Immature neuron numbers estimated on Nissl-stained sections. (*B*) Rostrocaudal distributions of immature neurons in the different groups (left = rostral, right = caudal; average ± SD). (*C*) Dorsoventral and mediolateral distribution of immature neurons in the different groups. (*D*) Illustration of $Bcl2^{+}$ cells in the paralaminar nucleus of the amygdala. Thin processes were visible around most of the labeled cells (black arrowheads). (Scale bar, 25 μm.) (*E*) Numbers of intensely labeled $Bcl2^{+}$ small cells in the paralaminar nucleus. See also Figs. S4 and S5.

small mature neurons in neonate-lesioned monkeys than in adult-lesioned and control monkeys ($P = 0.016$, $P = 0.002$). The number of small mature neurons did not differ between adult-lesioned and control monkeys ($P = 0.411$). Similarly, the number of neurons larger than the controls' median neuron size differed between groups (Fig. 5*D*) [$F_{(2,\ 18)} = 5.658$, $P = 0.012$). There were more large mature neurons in neonate-lesioned monkeys than in adult-lesioned and control monkeys ($P = 0.018$, $P = 0.007$). The number of large mature neurons did not differ between adult-lesioned and control monkeys ($P = 0.738$).

Basal nucleus. The average volume of mature neuron somas differed between groups in the basal nucleus (Fig. 5*E*) [$F_{(2,\ 18)} = 3.698$, $P = 0.045$]. The average volume of mature neuron somas was 8% smaller in neonate-lesioned monkeys than in controls ($P = 0.036$) and 10% smaller in adult-lesioned monkeys than in controls ($P = 0.026$). In addition, the number of neurons smaller than the controls' median neuron size differed between groups (Fig. 5*F*) [$F_{(2,\ 18)} = 8.048$, $P = 0.003$]. There were more small mature neurons in neonate-lesioned monkeys than in adult-lesioned and control monkeys ($P = 0.007$, $P = 0.002$). The number of small mature neurons did not differ between adult-lesioned and control monkeys ($P = 0.604$). Similarly, the number of neurons larger than the controls' median neuron size differed between groups (Fig. 5*F*) [$F_{(2,\ 18)} = 5.483$, $P = 0.014$]. There were more large mature neurons in neonate-lesioned monkeys than in adult-lesioned monkeys ($P = 0.004$). In contrast, the number of large mature neurons did not differ between control and neonate- or adult-lesioned monkeys ($P = 0.115$, $P = 0.113$).

Discussion

We have shown that hippocampal lesions lead to an increase in the number of mature neurons in the amygdala of adult monkeys, which appears to reflect the differentiation of immature neurons present in the paralaminar nucleus. After neonatal lesions, the differentiation of immature neurons involved the paralaminar, lateral, and basal nuclei, and was associated with an increase in the population of immature neurons in the paralaminar nucleus. In contrast, after adult lesions, the differentiation of immature neurons was essentially restricted to the paralaminar nucleus and was associated with a decrease in the population of immature neurons.

Differentiation of Immature Neurons.

Neonatal hippocampal lesion. The increase in mature neuron numbers in the paralaminar, lateral, and basal nuclei observed in neonate-lesioned monkeys suggested that immature neurons may have migrated from the paralaminar nucleus to integrate into other amygdala nuclei. This hypothesis is consistent with a report showing $Bcl2^{+}$ cells and fibers extending dorsally from the paralaminar nucleus into the lateral and basal nuclei (3). In parallel, we observed an increase in the number of immature neurons in the paralaminar nucleus following neonatal hippocampal lesion. Although the existence of adult-generated neurons in the monkey amygdala has been suggested (12), there is no indication that these neurons are born from the division of in situ progenitor cells within the amygdala (12, 36). Instead, it has been suggested that the migration of neuroblasts from the subventricular zone may contribute to the integration of postnatally generated neurons into the amygdala (12). Although no definitive proof of this putative migratory route has been provided by previous studies (12, 36), or by our current results, it is a plausible hypothesis to account for the increase in the number of immature neurons in the paralaminar nucleus following neonatal lesion of the hippocampus.

Adult hippocampal lesion. Following adult hippocampal lesion, the increase in mature neuron number in the paralaminar nucleus appeared to be largely associated with the maturation of immature neurons already present in the amygdala, because the number of immature neurons in the paralaminar nucleus was decreased, compared with controls. However, the total number of immature and mature neurons was slightly higher in adult-lesioned monkeys than in controls, suggesting that a small number of neurons may have been added to the amygdala possibly through migration from

http://doc.rero.ch

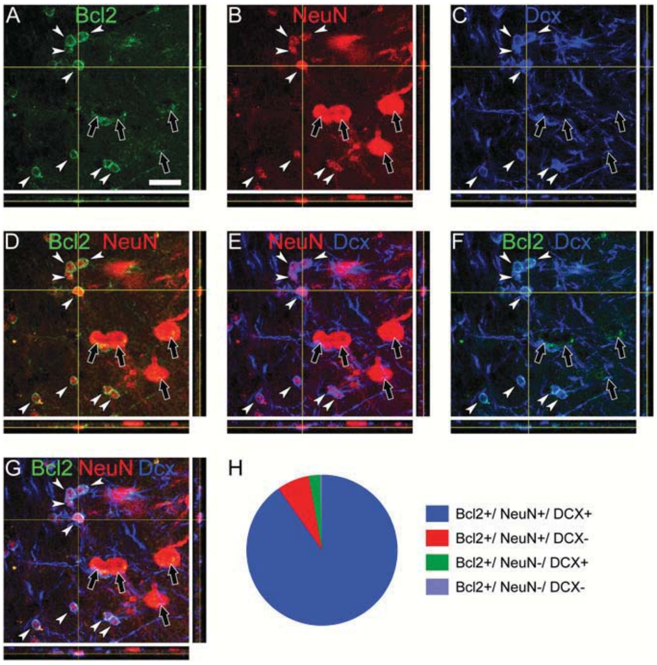

Fig. 4. Neuron phenotypes. Confocal images of $Bcl2^+$, $NeuN^+$, and DCX^+ cells in the monkey ventromedial amygdala. (*A*) Bcl2 staining. (*B*) NeuN staining. (*C*) DCX staining. (*D*) Bcl2/NeuN staining. (*E*) NeuN/DCX staining. (*F*) Bcl2/DCX staining. (*G*) Bcl2/NeuN/DCX staining. White arrowheads: immature neurons ($Bcl2^+/NeuN^+/DCX^+$). Black arrows: mature neurons ($Bcl2^-/NeuN^+/DCX^-$). (Scale bar for *A*–*G*, 20 μm.) (*H*) Percentages of $Bcl2^+$ cells expressing NeuN or DCX. Blue: 90% of $Bcl2^+$ cells expressed both NeuN and DCX. Red: 7% of $Bcl2^+$ cells expressed NeuN but not DCX. Green: 3% of $Bcl2^+$ cells expressed DCX but not NeuN. Purple: 0.4% of $Bcl2^+$ cells did not express NeuN or DCX. See Figs. S6 and S7 for additional information regarding the distinction between mature and immature neurons.

the subventricular zone in adulthood. This hypothesis would be consistent with previous findings reporting the migration of neuroblasts from the subventricular zone to the amygdala in adult unlesioned monkeys (12). If so, it is possible that cell proliferation in the subventricular zone and neuroblast migration toward the amygdala was up-regulated in adult hippocampal-lesioned monkeys, but to a much lesser extent than following neonatal hippocampal lesions. In sum, it appears that the increase in mature neuron numbers in the monkey paralaminar nucleus following adult hippocampal lesion is largely a result of the maturation of immature neurons already present in this nucleus.

Nonexperimental hippocampal lesion. In one monkey with a nonexperimental hippocampal lesion (NEHL1), increases in mature neuron numbers in the paralaminar, lateral, and basal nuclei were similar to those in experimental neonate-lesioned monkeys. In a second monkey with a nonexperimental lesion (NEHL2), however, changes in mature neuron numbers in the paralaminar nucleus were similar to those observed in adult-lesioned monkeys. This finding suggests that the hippocampal damage in NEHL1 may have occurred early in life, whereas hippocampal damage in NEHL2 may have occurred during adulthood. The hypothesis that in NEHL2 hippocampal damage occurred during adulthood is consistent with previous behavioral observations, which revealed that NEHL2 exhibited spatial memory deficits similar to adult experimental hippocampal-lesioned monkeys (23). Findings from these two animals presenting nonexperimental restricted hippocampal lesions support the link between hippocampal dysfunction and changes in neuron numbers in the amygdala. See *SI Results* for more information.

Lesion-Induced Plasticity. The major finding of the current study is that the differentiation of immature neurons in the adult monkey amygdala may be up-regulated by a focal lesion affecting a different, but functionally related, brain region. Indeed, the hippocampal formation has many monosynaptic connections with several amygdala nuclei, including those that have shown changes in neuron number (18–21).

Although lesion-induced migration of neurons was previously suggested in primates (7, 9, 37), the integration of these neurons was never quantified and appeared to be limited to the immediate area surrounding the lesion site. Because of the existence of a local population of immature neurons and the evidence that many of them mature in the course of postnatal development (10), the amygdala may be a particularly favorable environment for the integration of immature neurons into functional circuits. Why the amygdala appears to have this privileged regenerative potential remains to be determined. Although we did not have the possibility to directly determine the proportion of immature neurons that matured and survived, we can speculate that most of them survived, because the

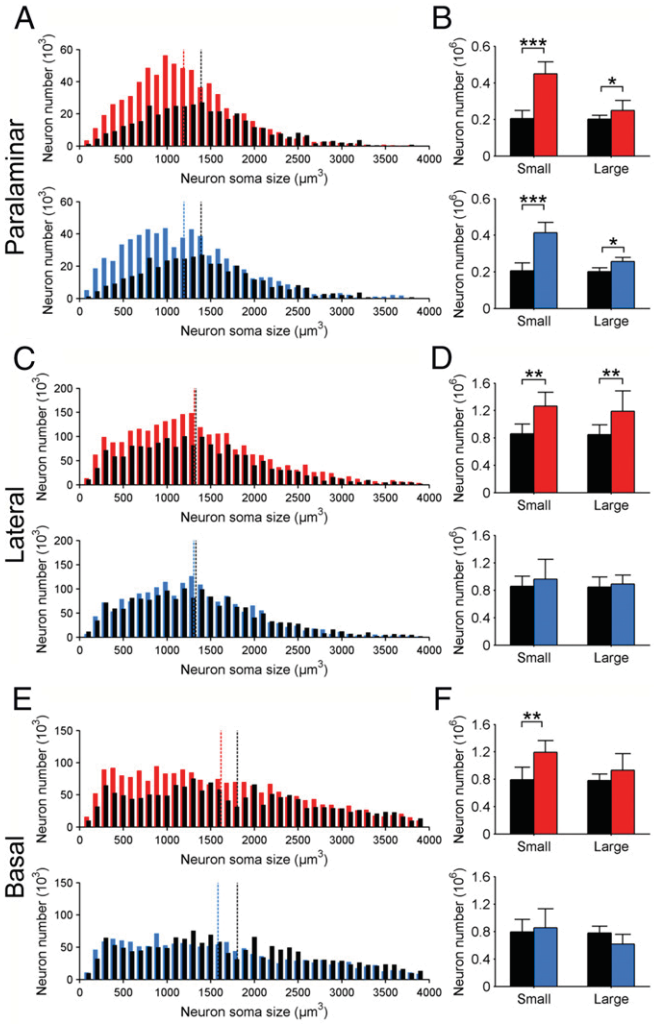

Fig. 5. Soma size. (*A*, *C*, and *E*) Distribution of mature neuron soma size (in cubic micrometers, μm^3) in unoperated control (black), neonatal hippocampal-lesioned (red), and adult hippocampal-lesioned (blue) monkeys. Dashed vertical lines indicate the median for each group. (*A*) Paralaminar nucleus. (*C*) Lateral nucleus. (*E*) Basal nucleus. (*B*, *D*, and *F*) Number of neurons with a soma size smaller or larger than the median neuron size estimated in controls. (*B*) Paralaminar nucleus. (*D*) Lateral nucleus. (*F*) Basal nucleus. (Average ± SD; $*P < 0.05$; $**P < 0.01$; $***P < 0.001$). See also *SI Experimental Procedures* and *SI Results*.

number of mature plus immature neurons in the paralaminar nucleus of adult-lesioned monkeys was slightly higher than in controls.

Increased differentiation of neurons in the amygdala might have been triggered by hippocampal dysfunction, and not necessarily by the release of trophic factors following experimental lesions. Indeed, even though neonatal, ibotenic acid lesion of the ventral hippocampus leads to persistent astrogliosis and microglial activation associated with the production of inflammatory mediators (38, 39), the diffusion of apoptosis-related signals is unlikely to explain the strikingly similar patterns of changes observed in monkeys with nonexperimental, restricted hippocampal lesions. This finding suggests that impaired hippocampal function may be primarily responsible for the neuronal plasticity observed in the amygdala. Accordingly, we observed a global decrease of the average neuronal soma size in the paralaminar nucleus of neonate- and adult-lesioned animals, and in the basal nucleus of neonate-lesioned monkeys. In contrast, the distribution of neuronal soma size was the same as in controls in the lateral nucleus of neonate- and adult-lesioned monkeys. Interestingly, both the paralaminar and the ventral part of the basal nucleus, but not the lateral nucleus, have reciprocal connections with CA1 and the subiculum; the lateral nucleus has reciprocal projections with the rostral entorhinal cortex (18–21), which was intact in all experimental monkeys. The decrease in average neuron soma size may thus reflect the shrinkage of amygdala neurons that normally interact with hippocampal neurons, as was shown in other brain regions (40, 41). The decrease in average neuron soma size may also reflect the fact that newly maturing neurons did not establish the same complement of connections as the preexisting neurons, and thus remained smaller than neurons already present in the amygdala that normally establish long distance connections, as is observed in other brain regions (7). This hypothesis is consistent with the fact that the size of a developing neuron soma is related to the length of its projection and its level of connectivity (42).

Conclusion

Our quantitative estimates of neuron numbers and phenotypes demonstrated the potential for immature neurons to differentiate into mature neurons following focal brain damage. Specifically, we showed that hippocampal lesions lead to an increase in mature neuron numbers in the adult monkey amygdala. Such lesion-induced plasticity sheds new light on potential mechanisms that may facilitate functional recovery following focal brain injury.

ACKNOWLEDGMENTS. This work was supported in part by Swiss National Science Foundation Grants P00A-106701, PP00P3-124536, and 310030_143956; US NIH Grants MH041479 and NS16980; and California National Primate Research Center Grant OD011107.

1. Bernier PJ, Parent A (1998) Bcl-2 protein as a marker of neuronal immaturity in postnatal primate brain. *J Neurosci* 18(7):2486–2497.
2. Bloch J, et al. (2011) Doublecortin-positive cells in the adult primate cerebral cortex and possible role in brain plasticity and development. *J Comp Neurol* 519(4):775–789.
3. Fudge JL (2004) Bcl-2 immunoreactive neurons are differentially distributed in subregions of the amygdala and hippocampus of the adult macaque. *Neuroscience* 127(2):539–556.
4. Nacher J, Crespo C, McEwen BS (2001) Doublecortin expression in the adult rat telencephalon. *Eur J Neurosci* 14(4):629–644.
5. Yachnis AT, Roper SN, Love A, Fancey JT, Muir D (2000) Bcl-2 immunoreactive cells with immature neuronal phenotype exist in the nonepileptic adult human brain. *J Neuropathol Exp Neurol* 59(2):113–119.
6. Arvidsson A, Collin T, Kirik D, Kokaia Z, Lindvall O (2002) Neuronal replacement from endogenous precursors in the adult brain after stroke. *Nat Med* 8(9):963–970.
7. Tonchev AB, Yamashima T, Sawamoto K, Okano H (2005) Enhanced proliferation of progenitor cells in the subventricular zone and limited neuronal production in the striatum and neocortex of adult macaque monkeys after global cerebral ischemia. *J Neurosci Res* 81(6):776–788.
8. Darsalia V, Heldmann U, Lindvall O, Kokaia Z (2005) Stroke-induced neurogenesis in aged brain. *Stroke* 36(8):1790–1795.
9. Jin K, et al. (2006) Evidence for stroke-induced neurogenesis in the human brain. *Proc Natl Acad Sci USA* 103(35):13198–13202.
10. Chareyron LJ, Lavenex PB, Amaral DG, Lavenex P (2012) Postnatal development of the amygdala: A stereological study in macaque monkeys. *J Comp Neurol* 520(9):1965–1984.
11. deCampo DM, Fudge JL (2012) Where and what is the paralaminar nucleus? A review on a unique and frequently overlooked area of the primate amygdala. *Neurosci Biobehav Rev* 36(1):520–535.
12. Bernier PJ, Bedard A, Vinet J, Levesque M, Parent A (2002) Newly generated neurons in the amygdala and adjoining cortex of adult primates. *Proc Natl Acad Sci USA* 99(17):11464–11469.
13. Fudge JL, deCampo DM, Becoats KT (2012) Revisiting the hippocampal-amygdala pathway in primates: Association with immature-appearing neurons. *Neuroscience* 212:104–119.
14. Marlatt MW, et al. (2011) Distinct structural plasticity in the hippocampus and amygdala of the middle-aged common marmoset (*Callithrix jacchus*). *Exp Neurol* 230(2):291–301.
15. Zhang XM, et al. (2009) Doublecortin-expressing cells persist in the associative cerebral cortex and amygdala in aged nonhuman primates. *Front Neuroanat* 3:17.
16. Lim DA, Alvarez-Buylla A (2014) Adult neural stem cells stake their ground. *Trends Neurosci* 37(10):563–571.
17. Christie KJ, Turnley AM (2013) Regulation of endogenous neural stem/progenitor cells for neural repair-factors that promote neurogenesis and gliogenesis in the normal and damaged brain. *Front Cell Neurosci* 6:70.
18. Amaral DG, Price JL, Pitkanen A, Carmichael T (1992) Anatomical organization of the primate amygdaloid complex. *The Amygdala: Neurobiological Aspects of Emotion, Memory, and Mental Dysfunction*, ed Aggleton J (Wiley-Liss, New York), pp 1–66.
19. Rosene DL, Van Hoesen GW (1977) Hippocampal efferents reach widespread areas of cerebral cortex and amygdala in the rhesus monkey. *Science* 198(4314):315–317.
20. Aggleton JP (1986) A description of the amygdalo-hippocampal interconnections in the macaque monkey. *Exp Brain Res* 64(3):515–526.
21. Saunders RC, Rosene DL, Van Hoesen GW (1988) Comparison of the efferents of the amygdala and the hippocampal formation in the rhesus monkey: II. Reciprocal and non-reciprocal connections. *J Comp Neurol* 271(2):185–207.
22. Bauman MD, Lavenex P, Mason WA, Capitanio JP, Amaral DG (2004) The development of mother-infant interactions after neonatal amygdala lesions in rhesus monkeys. *J Neurosci* 24(3):711–721.
23. Lavenex PB, Amaral DG, Lavenex P (2006) Hippocampal lesion prevents spatial relational learning in adult macaque monkeys. *J Neurosci* 26(17):4546–4558.
24. Jabès A, Lavenex PB, Amaral DG, Lavenex P (2010) Quantitative analysis of postnatal neurogenesis and neuron number in the macaque monkey dentate gyrus. *Eur J Neurosci* 31(2):273–285.
25. Jabès A, Lavenex PB, Amaral DG, Lavenex P (2011) Postnatal development of the hippocampal formation: A stereological study in macaque monkeys. *J Comp Neurol* 519(6):1051–1070.
26. Chareyron LJ, Banta Lavenex P, Amaral DG, Lavenex P (2011) Stereological analysis of the rat and monkey amygdala. *J Comp Neurol* 519(16):3218–3239.
27. Bauman MD, Lavenex P, Mason WA, Capitanio JP, Amaral DG (2004) The development of social behavior following neonatal amygdala lesions in rhesus monkeys. *J Cogn Neurosci* 16(8):1388–1411.
28. Lavenex P, Lavenex PB, Amaral DG (2007) Spatial relational learning persists following neonatal hippocampal lesions in macaque monkeys. *Nat Neurosci* 10(2):234–239.
29. Moadab G, Bliss-Moreau E, Amaral DG (2015) Adult social behavior with familiar partners following neonatal amygdala or hippocampus damage. *Behav Neurosci* 129(3):339–350.
30. Lavenex P, Lavenex PB, Bennett JL, Amaral DG (2009) Postmortem changes in the neuroanatomical characteristics of the primate brain: Hippocampal formation. *J Comp Neurol* 512(1):27–51.
31. Mullen RJ, Buck CR, Smith AM (1992) NeuN, a neuronal specific nuclear protein in vertebrates. *Development* 116(1):201–211.
32. Francis F, et al. (1999) Doublecortin is a developmentally regulated, microtubule-associated protein expressed in migrating and differentiating neurons. *Neuron* 23(2):247–256.
33. Brown JP, et al. (2003) Transient expression of doublecortin during adult neurogenesis. *J Comp Neurol* 467(1):1–10.
34. Gundersen HJG, Jensen EB (1987) The efficiency of systematic sampling in stereology and its prediction. *J Microsc* 147(Pt 3):229–263.
35. Carmer SG, Swanson MR (1973) Evaluation of 10 pairwise multiple comparison procedures by Monte-Carlo methods. *J Am Stat Assoc* 68(341):66–74.
36. Rakic P (2002) Neurogenesis in adult primate neocortex: An evaluation of the evidence. *Nat Rev Neurosci* 3(1):65–71.
37. Shen J, et al. (2008) Neurogenesis after primary intracerebral hemorrhage in adult human brain. *J Cereb Blood Flow Metab* 28(8):1460–1468.
38. Drouin-Ouellet J, et al. (2011) Neuroinflammation is associated with changes in glial mGluR5 expression and the development of neonatal excitotoxic lesions. *Glia* 59(2): 188–199.
39. Vázquez-Roque RA, et al. (2012) Chronic administration of the neurotrophic agent cerebrolysin ameliorates the behavioral and morphological changes induced by neonatal ventral hippocampus lesion in a rat model of schizophrenia. *J Neurosci Res* 90(1):288–306.
40. Beaud ML, et al. (2008) Anti-Nogo-A antibody treatment does not prevent cell body shrinkage in the motor cortex in adult monkeys subjected to unilateral cervical cord lesion. *BMC Neurosci* 9:5.
41. Wannier T, Schmidlin E, Bloch J, Rouiller EM (2005) A unilateral section of the corticospinal tract at cervical level in primate does not lead to measurable cell loss in motor cortex. *J Neurotrauma* 22(6):703–717.
42. Ngwenya LB, Peters A, Rosene DL (2006) Maturational sequence of newly generated neurons in the dentate gyrus of the young adult rhesus monkey. *J Comp Neurol* 498(2):204–216.
43. Paxinos G, Huang X-F, Toga AW (1999) *The Rhesus Monkey Brain in Stereotaxic Coordinates* (Academic, San Diego, USA), 1st Ed.
44. Gundersen HJ (1988) The nucleator. *J Microsc* 151(Pt 1):3–21.

http://doc.rero.ch

Supporting Information

Chareyron et al. 10.1073/pnas.1604288113

SI Experimental Procedures

Animals and Lesion Surgeries. Twenty-three macaque monkeys (*Macaca mulatta*) were used for this study. Monkeys were naturally born from multiparous mothers and raised at the California National Primate Research Center. Experimental procedures were approved by the Institutional Animal Care and Use Committee of the University of California, Davis, and were conducted in accordance with the National Institutes of Health guidelines for the use of animals in research. To reduce the number of animals used for research, all monkeys had been involved in other studies before being recruited for this study.

Unoperated control monkeys (n = 7). Four adult monkeys (5.3–9.4 y) were used in quantitative studies of the monkey hippocampal formation (24, 25) and amygdala (10, 26). These subjects were maternally reared in 2,000-m^2 outdoor enclosures and lived in large social groups until they were killed. Four monkeys (9.2–9.5 y) were added to serve as unoperated controls for the current study. They were maternally reared in 2,000-m^2 outdoor enclosures and lived in large social groups until their recruitment for this study, approximately 3 mo before brain acquisition, when they were moved into indoor cages (61-cm width × 66-cm depth × 81-cm height). One of these monkeys (NEHL1; 9.4 y) had a nonexperimental, selective lesion of the hippocampus and is thus considered separately in this study.

Neonatal hippocampal-lesioned monkeys (n = 8). These eight animals were part of a longitudinal study of the effects of neonatal damage to the amygdala or hippocampus on the development of social behavior. Comprehensive rearing history has been described previously (27–29). Briefly, infants were reared by their mothers in a socialization cohort consisting of six mother–infant pairs and one adult male. Infants were weaned from their mothers when the youngest member of each cohort reached 6 mo of age. Infants were then permanently housed with their previously established cohort of six infants, one adult male, and a new adult female. They were 9.1–9.4 y of age at the time their brains were collected.

Adult hippocampal-lesioned monkeys (n = 6). These six animals were used in a study of the role of the hippocampus in spatial learning in adult macaque monkeys (23). They were maternally reared in 2,000-m^2 outdoor enclosures and lived in large social groups until about one year before experimental lesion surgery (at 6–9 y of age). At that time, each monkey was moved indoors and maintained in a standard home cage. They were 10.6–13.4 y of age at the time their brains were collected. One additional monkey (NEHL2; 12.6 y) originally assigned to the study's control group had a nonexperimental, selective lesion of the hippocampus (23) and is thus considered separately in this study.

Experimental lesion surgeries. Bilateral hippocampal lesions were performed following the same protocol for both neonatal (12-16 d after birth) and adult (at 6.7–9.7 y of age) lesion groups. Detailed procedures are described in refs. 22 and 23.

Histological Processing.

Brain acquisition. Monkeys were deeply anesthetized with an intravenous injection of sodium pentobarbital (50 mg/kg; Fatal-Plus, Vortech Pharmaceuticals) and perfused transcardially with 1% and then 4% (wt/vol) paraformaldehyde in 0.1 M phosphate buffer (PB; pH 7.4) following standard protocols (30).

Nissl staining. One series of 30- or 60-μm sections were collected in 10% (wt/vol) formaldehyde solution in 0.1 M PB (pH 7.4) and postfixed at 4 °C for 4 wk before Nissl staining. Other series were collected in tissue collection solution (TCS) and kept at −70 °C until further processing. The procedure for Nissl-stained sections followed our standard laboratory protocol (30).

NeuN, Bcl2, DCX: Neuronal phenotype markers. We used three cell specific markers, NeuN, Bcl2, and DCX, to characterize the phenotypes of neurons in the ventromedial amygdala. NeuN is a well-established neuron-specific marker (31). Bcl2 is an antiapoptotic protein, which influences the rate of neuronal differentiation in young neurons and is expressed in populations of immature neurons (1). DCX is a well-defined marker of immature neurons (32, 33). Thirty-micrometer-thick sections were rinsed 3 × 10 min in 0.1 M PBS (pH 7.4), and incubated for 96 h in primary antiserum at 4 °C with gentle agitation on a rotating platform [1:50 mouse anti-Bcl2 (Abcam, Ab694) + 1:1,000 guinea-pig anti-NeuN (Merck Millipore, ABN90P) + 1:1,000 rabbit anti-DCX (Abcam, Ab18723) in 0.1 M PBS + 0.1% Triton X-100 + 10% (vol/vol) bovine serum (Pan Biotech, P30-0602)]. Sections were then rinsed 10 min in 0.1 M PBS, 2 × 10 min in Tris buffer, and incubated for 4 h at room temperature in secondary antiserum with gentle agitation on a rotating platform [1:400 Alexa Fluor 488-conjugated goat anti-mouse IgG (Thermo Fisher Scientific, A-11029) + 1:400 Alexa Fluor 568-conjugated goat anti–guinea-pig IgG (Thermo Fisher Scientific, A-11075) + 1:400 Alexa Fluor 647-conjugated goat anti-rabbit IgG (Thermo Fisher Scientific, A-21245) in Tris buffer]. From this point on, sections were protected from light. Sections were rinsed 10 min in Tris buffer, 2 × 10 min in 0.1 M PBS, mounted on gelatin-coated slides, and air-dried overnight at room temperature. Sections were dehydrated through a graded series of ethanol solutions and coverslipped with DPX new (Merck KGaA, 100579).

Bcl2: Immature neuron marker. We used Bcl2 immunohistochemistry to label immature neurons and obtain a second estimate of immature neuron numbers. One series of 30-μm-thick sections (960-μm apart) was taken from TCS and rinsed for 3 × 5 min in 0.1 M PBS containing 0.2% Triton X-100 (PBST, pH 7.4; Sigma-Aldrich, 9002-93-1), incubated for 25 min in 0.3% H_2O_2 in PBST, rinsed for 4 × 5 min in 0.1 M PBST, and incubated for 4 h in a blocking solution comprised of 3% (vol/vol) normal horse serum (Chemie Brunschwig, UP24741C) in 0.1 M PBST at room temperature. Sections were then incubated for 96 h in primary antiserum (mouse anti-Bcl2; Abcam, Ab694; at 1:50 in 0.1 M PBST) at 4 °C, rinsed for 5 × 5 min at room temperature in 0.1 M PBST, incubated for 2 h in secondary antiserum (biotinylated horse anti-mouse IgG; Vector Laboratories, BA-2000; at 1:250 in 0.1 M PBST), rinsed for 5 × 5 min in 0.1 M PBST, incubated for 1.5 h in avidin-biotin complex (HRP-Basic IHC kit, ImmunoBioScience, 8106) in 0.1 M PBST at room temperature, rinsed for 3 × 5 min in 0.1 M PBST, rinsed for 2 × 5 min in 0.05 M Tris buffer and incubated for 1 h in a 0.05% diaminobenzidine (Sigma-Aldrich, D5905) /0.04% H_2O_2 solution. Sections were then rinsed, mounted onto gelatin-coated slides, defatted and coverslipped with DPX new.

Data Acquisition and Statistical Analyses.

Stereological analyses on Nissl-stained sections. We used the optical fractionator method (34) on Nissl-stained sections to estimate the numbers of mature and immature neurons in the paralaminar, lateral, and basal nuclei of the amygdala (Tables S1 and S2). Neuron number was estimated in the right or left amygdala, as determined pseudorandomly for each individual. For each amygdala nucleus, we used about 11 sections per animal (480-μm apart), with the first section selected randomly within the first two sections through the nucleus of interest. We used a 100× Plan Fluor oil objective (N.A. 1.30) on a Nikon Eclipse 80i microscope (Nikon Instruments) linked to PC-based StereoInvestigator

http://doc.rero.ch

http://doc.rero.ch

11.0 (MBF Bioscience). The sampling scheme was adapted for each nucleus to obtain individual estimates with coefficients of error (CE) around 0.10 [CE average (mature neurons) = 0.099; CE average (immature neurons) = 0.119]. Section thickness was measured at every other counting site. The volume of neuronal somas, of every neuron counted during the optical fractionator analysis, was determined using the nucleator method (44). We distinguished mature and immature neurons from other cells, based on morphological criteria identifiable in Nissl preparations (10, 26). Briefly, neurons are darkly stained and comprise a single large nucleolus. Immature neurons are small with round to slightly oval, hyperchromatic nuclei containing distinguishable nucleoli (3, 5, 12).

Stereological analyses on Bcl2-labeled sections. We used the optical fractionator method to estimate the number of Bcl2-labeled immature neurons in the paralaminar nucleus (Tables S1 and S2). Cell number was estimated in the right or in the left amygdala only. We used about six sections per animal (960-μm apart), with the first section selected randomly within the first two sections through the paralaminar nucleus. Section thickness was measured at every counting site. This sampling scheme was established to obtain individual estimates with CE around 0.10 [CE average ($Bcl2^+$ cells) = 0.167].

Neuronal phenotypes. We used a confocal microscope (TCS SP5, DM6000 CFS, Leica Microsystems) to determine the phenotype of immature neurons in the ventromedial amygdala, based on the colocalization of Bcl2, NeuN, and DCX (Fig. 4 and Fig. S6). We used a 40× objective corrected for chromatic and spherical aberration (HC PL APO 40×/1.30 oil CS2) and performed a sequential acquisition to avoid “cross-talk” between different excitation lasers and photomultiplier detection systems. Bcl2 visualization (fluorophore Alexa Fluor 488): excitation: 488 nm (argon laser); detection: 505–539 nm, gain 711, offset −1.2, pinhole 1.93 AU/126 μm. NeuN visualization (fluorophore Alexa Fluor 568): excitation: 561 nm (DPSS laser); detection: 585–624 nm, gain 805, offset 0.7, pinhole 1.93 AU/126 μm. DCX visualization (fluorophore Alexa Fluor 647): excitation: 633 nm (HeNe laser); detection: 658–688 nm, gain 728, offset 1.6, pinhole 1.93 AU/126 μm. For each acquisition, we used z-steps of 0.5 μm. We analyzed a total of about 550 $Bcl2^+$ cells (about 25 $Bcl2^+$ cells per animal) using Fiji/ImageJ software v1.50b (NIH). The percentage of $Bcl2^+$ cells expressing NeuN or DCX were calculated for each experimental condition.

Illustrations. The mediolateral and dorsoventral distributions of mature and immature neurons are presented on cell-density maps derived from stereological analyses data. For each monkey, all coronal sections analyzed for each nucleus were aligned along the same axis, centered, stacked, and then summed. We then normalized the x and y dimensions of these maps (i.e., the height and width of the nuclei) to produce an average map for each experimental group. We used an arbitrary color scale to illustrate group differences. Low-magnification photomicrographs of lesion extent were taken with a Leica DFC420 digital camera on a Leica MZ95 microscope (Leica Microsystems). High-magnification photomicrographs (Bcl2-labeled cells) were taken with a Qimaging Retiga-2000R digital camera (Qimaging) on a Nikon Eclipse 80i microscope (Nikon Instruments). Levels were adjusted in Adobe Photoshop CS6, v13.0 (Adobe) or Fiji/ImageJ software v1.50b (NIH).

SI Results

Neonatal Hippocampal Lesions. In neonate-lesioned monkeys, the volumes of the remaining dentate gyrus granule cell layer and hippocampal fields CA3, CA2, and CA1, measured on Nissl-stained sections (Fig. 1) were, respectively, 20%, 14%, 15%, and 23% of that of the controls. The volumes of the subiculum, presubiculum, and parasubiculum were, respectively, 13%, 27%, and 57% of that of the controls. Portions of the parahippocampal cortex were also damaged and its average volume in neonate-lesioned monkeys was 75% of that of the controls. The entorhinal and perirhinal cortices were entirely preserved (102% and 115% of controls, respectively). The medial portion of cortical areas TEO and V4 sustained restricted damage in some monkeys.

Adult Hippocampal Lesions. Lesion extent has been described in ref. 23. Briefly, the volumes of the remaining dentate gyrus granule cell layer and hippocampal fields CA3, CA2, and CA1, measured on Nissl-stained sections (Fig. 1), were, respectively, 30%, 46%, 10%, and 14% of that of the controls. The volumes of the subiculum, presubiculum, and parasubiculum were respectively 15%, 18%, and 47% of that of the controls. Portions of the parahippocampal cortex were damaged and its average volume was 37% of that of the controls. The entorhinal and perirhinal cortices were largely preserved (89% and 123% of that of the controls, respectively). The medial portion of area TEO (from the border with area TFl to the fundus of the occipito temporal sulcus) sustained restricted damage in some monkeys. A portion of area V4 located directly below the hippocampus was damaged in all monkeys.

Nonexperimental Hippocampal Lesions. Two monkeys (NEHL1 and NEHL2) had nonexperimental, selective, bilateral damage to the dentate gyrus or hippocampus. Their lesion condition was unknown when they were enrolled in these experiments. Their life history is described with that of the unoperated control and adult hippocampal-lesioned monkeys, respectively.

NEHL1 exhibited structural abnormalities in the caudal hippocampus in both hemispheres, including granule cell dispersion in the molecular layer of the dentate gyrus, granule cell loss, and gliosis (Fig. S1). In contrast, the volumes of the medial temporal lobe structures were larger than in controls: hippocampus + subicular complex [139% of controls’, $t_{(6)} = 3.182$; $P = 0.006$], entorhinal cortex [137%, $t_{(6)} = 3.211$; $P = 0.005$], perirhinal cortex [159%, $t_{(6)} = 3.974$; $P = 0.001$]. The volume of the parahippocampal cortex did not differ from that of controls [125%, $t_{(6)} = 1.771$; $P = 0.096$].

The extent of hippocampal damage in NEHL2 was described in ref. 28. Only the CA3, CA2, and CA1 fields of the hippocampus exhibited neuronal damage. Pyramidal neuron loss, gliosis, and cell reorganization occupied 21% of the rostrocaudal extent of the left hippocampus, and about 31% of the rostrocaudal extent of the right hippocampus.

http://doc.rero.ch

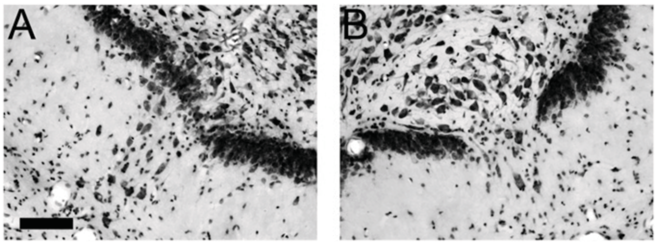

Fig. S1. Nissl-stained sections of an adult monkey with nonexperimental, selective lesion of the hippocampus: NEHL1. (*A*) Right hemisphere (Bregma −22.7). (*B*) Left hemisphere (Bregma −22.5). (Scale bar for both panels, 100 μm.)

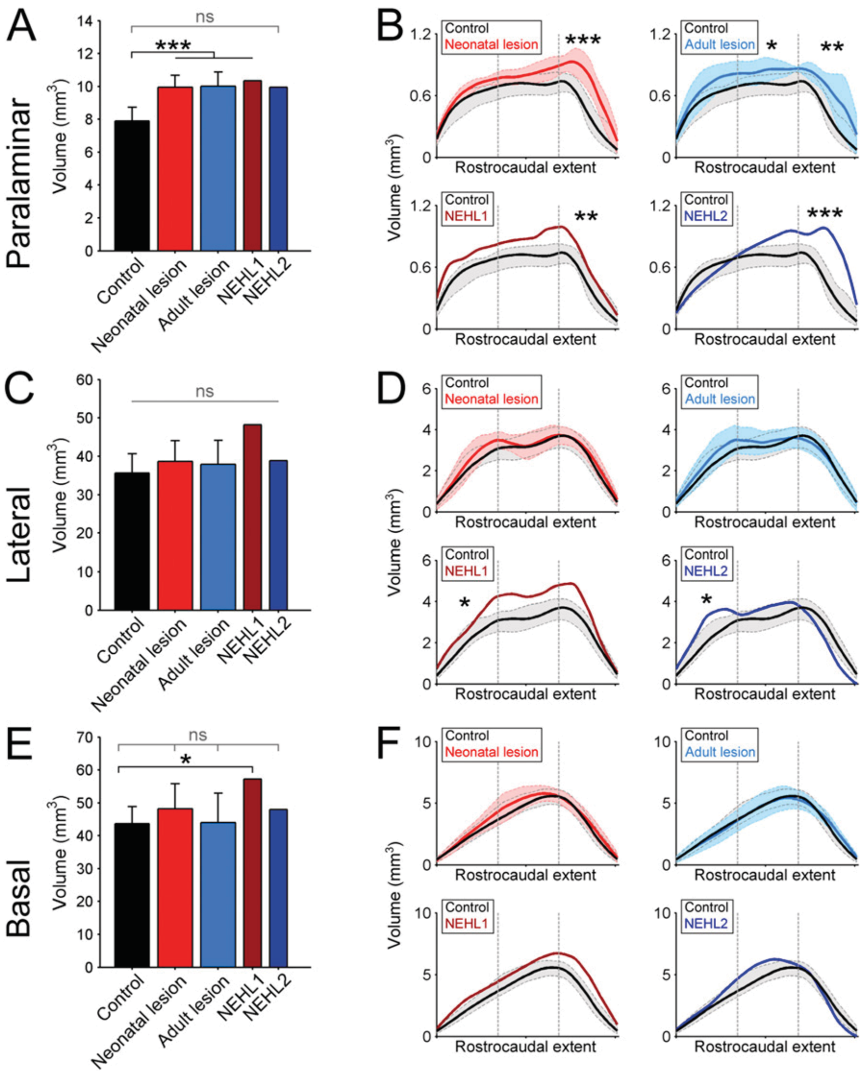

Fig. S2. Volumes and rostrocaudal profiles of the paralaminar, lateral, and basal nuclei of the amygdala of unoperated control (black), neonatal hippocampal-lesioned (red), adult hippocampal-lesioned (blue) monkeys, and two nonexperimental hippocampal-lesioned cases, NEHL1 (dark red) and NEHL2 (dark blue) (average ± SD; ns: not significant; *$P < 0.05$; **$P < 0.01$; ***$P < 0.001$). (*A* and *B*) Paralaminar nucleus. (*C* and *D*) Lateral nucleus. (*E* and *F*) Basal nucleus. (*A*, *C*, and *E*) Volumes. (*B*, *D*, and *F*) Rostrocaudal profiles of the amygdala nuclei in the different groups (left = rostral, right = caudal; average ± SD).

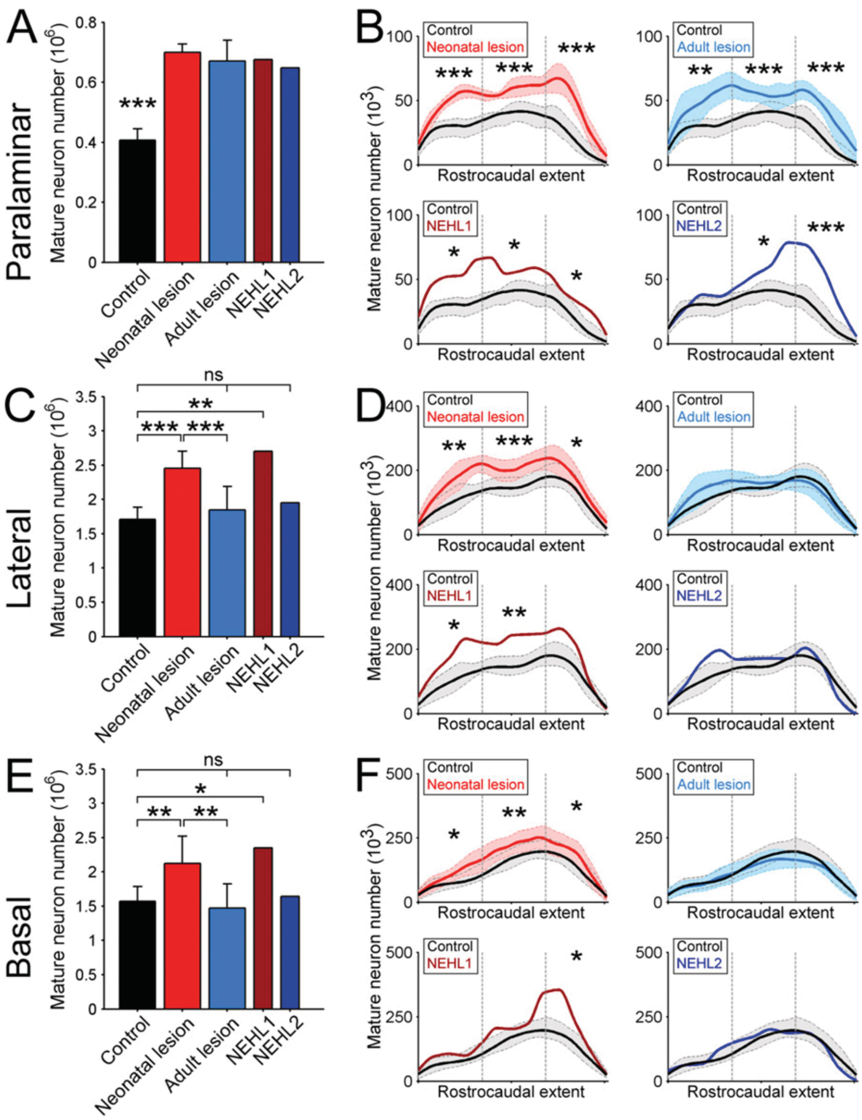

Fig. S3. Numbers and distributions of mature neurons in the amygdala nuclei of unoperated control (black), neonatal hippocampal-lesioned (red), adult hippocampal-lesioned (blue) monkeys, and two nonexperimental hippocampal-lesioned cases, NEHL1 (dark red) and NEHL2 (dark blue) (average ± SD; ns: not significant; *$P < 0.05$; **$P < 0.01$; ***$P < 0.001$). (*A* and *B*) Paralaminar nucleus. (*C* and *D*) Lateral nucleus. (*E* and *F*) Basal nucleus. (*A*, *C*, and *E*) Neuron numbers. (*B*, *D*, and *F*) Rostrocaudal distributions of mature neurons in the different groups (left = rostral, right = caudal; average ± SD).

http://doc.rero.ch

http://doc.rero.ch

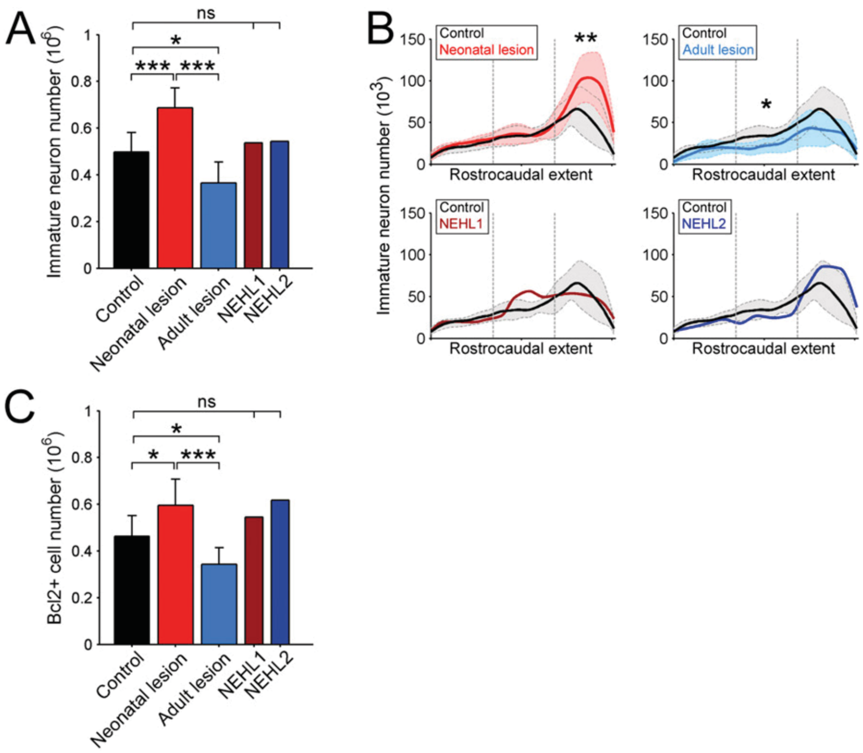

Fig. S4. Numbers and distributions of immature neurons in the paralaminar nucleus of unoperated control (black), neonatal hippocampal-lesioned (red), adult hippocampal-lesioned (blue) monkeys, and two nonexperimental hippocampal-lesioned cases, NEHL1 (dark red) and NEHL2 (dark blue). (Average ± SD; ns: not significant; $*P < 0.05$; $**P < 0.01$; $***P < 0.001$). (*A*) Immature neuron numbers estimated on Nissl-stained sections. (*B*) Rostrocaudal distributions of immature neurons in the different groups (left = rostral, right = caudal; average ± SD). (*C*) Bcl2$^+$ cell numbers.

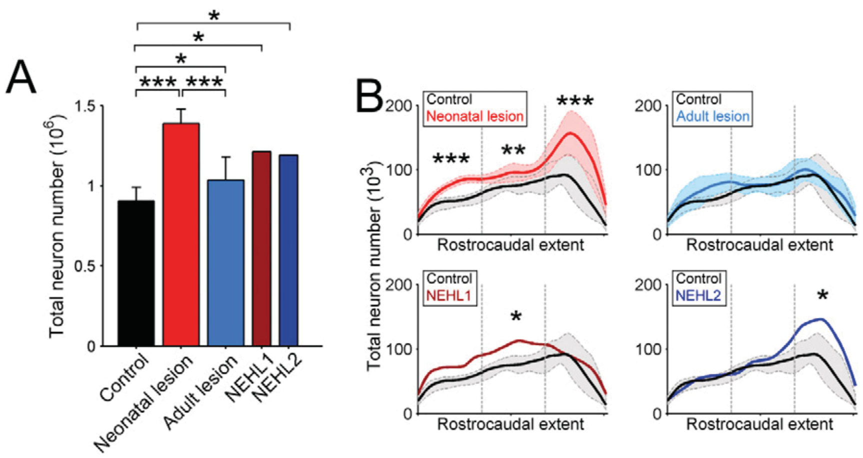

Fig. S5. Numbers and distributions of total number of neurons (mature + immature) in the paralaminar nucleus of unoperated control (black), neonatal hippocampal-lesioned (red), adult hippocampal-lesioned (blue) monkeys, and two nonexperimental hippocampal-lesioned cases NEHL1 (dark red) and NEHL2 (dark blue) (average ± SD; ns: not significant; $*P < 0.05$; $**P < 0.01$; $***P < 0.001$). (*A*) Total neuron numbers estimated on Nissl-stained sections. (*B*) Rostrocaudal distributions of the total number of neurons in the different groups (left = rostral, right = caudal; average ± SD).

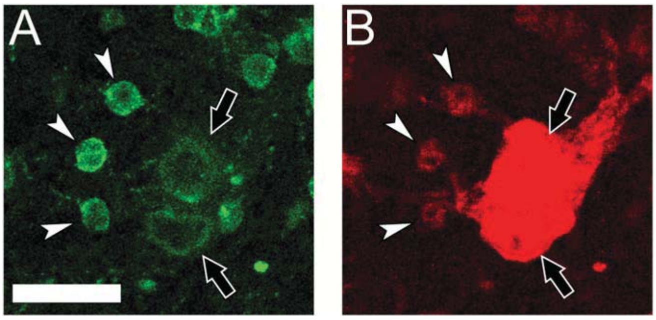

Fig. S6. Neuronal expression of Bcl2 in the paralaminar nucleus of the monkey amygdala. (*A*) Bcl2 staining. (*B*) NeuN staining. White arrowheads: immature neurons. Black arrows: mature neurons. (Scale bar for both *A* and *B*, 10 μm.)

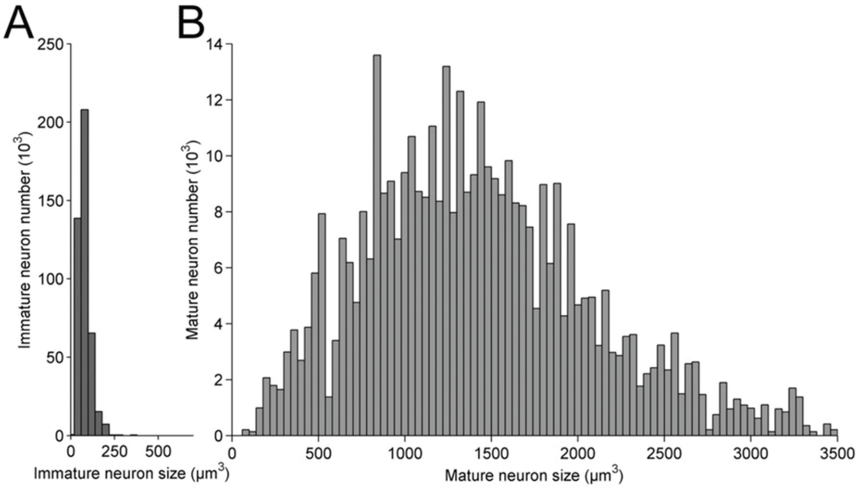

Fig. S7. Distributions of neuronal soma sizes in the paralaminar nucleus of the amygdala of unoperated-control monkeys. (*A*) Immature neurons. (*B*) Mature neurons.

http://doc.rero.ch

http://doc.rero.ch

Table S1. Sampling scheme used for cell counts

Staining	Cutting thickness (μm)	Condition	Amygdala nucleus	Average number of sections (range)	Distance between sections (μm)	Scan grid (μm)*	Counting frame (μm)	Disector height (μm)	Guard zones (μm)	Average section thickness (μm)†	Average number of neurons counted (range)	
											Mature	Immature
Nissl	60	Control (n = 4)	Lateral	11.5 (11–12)	480	600 × 600	40 × 40	5	2	13.9 (12.5–14.8)	322 (282–393)	
			Basal	11.0 (10–12)	480	550 × 550	40 × 40	5	2	14.6 (13.4–15.7)	329 (300–370)	
			Paralaminar	12.5 (11–13)	480	250 × 250	20 × 20	5	2	12.9 (12.0–13.6)	127 (107–137)	170 (135–198)
		Adult lesion‡ (n = 7)	Lateral	11.1 (9–12)	480	600 × 600	40 × 40	5	2	13.2 (12.6–14.5)	390 (289–441)	
			Basal	10.9 (9–12)	480	550 × 550	40 × 40	5	2	13.5 (12.7–14.6)	366 (211–435)	
			Paralaminar	11.4 (10–12)	480	250 × 250	20 × 20	5	2	13.0 (12.0–14.2)	205 (175–242)	121 (75–170)
	30	Control (n = 3)	Lateral	9.7 (9–10)	480	450 × 450	40 × 40	3	2	9.9 (8.0–11.5)	284 (253–342)	
			Basal	9.7 (9–10)	480	450 × 450	40 × 40	3	2	9.9 (7.9–11.4)	265 (250–292)	
			Paralaminar	10.7 (10–11)	480	200 × 200	40 × 40	3	2	8.9 (7.5–10.1)	347 (320–399)	375 (330–459)
		Neonatal lesion§ (n = 9)	Lateral	12 (10–14)	480	450 × 450	40 × 40	3	2	9.6 (7.5–10.7)	391 (291–562)	
			Basal	11.8 (11–13)	480	450 × 450	40 × 40	3	2	9.6 (7.8–10.8)	338 (197–521)	
			Paralaminar	12.4 (11–14)	480	200 × 200	40 × 40	3	2	9.3 (7.7–10.6)	570 (480–657)	549 (394–729)
Bcl2	30	All (n = 23)	Paralaminar	6.0 (5–7)	960	225 × 225	40 × 40	4	1	7.2 (6.4–7.8)	NA	269 (137–424)

*Scan grid was placed in random orientation.
†Section thickness was measured at every other counting site.
‡Including NEHL2.
§Including NEHL1.

Table S2. Stereological estimates

Neurons and cell numbers	Paralaminar	Lateral	Basal
Mature neuron number			
Control	407,123 ± 37,270	1,706,444 ± 178,120	1,573,016 ± 212,939
Neonatal lesion	700,264 ± 27,369	2,454,814 ± 247,625	2,125,273 ± 395,511
Adult lesion	670,142 ± 69,897	1,847,354 ± 340,830	1,470,181 ± 353,532
NEHL1	675,982 ± 0	2,700,389 ± 0	2,351,411 ± 0
NEHL2	648,020 ± 0	1,949,696 ± 0	1,641,349 ± 0
Mature neuron soma volume (μm^3)			
Control	1,479 ± 68	1,430 ± 122	2,052 ± 91
Neonatal lesion	1,263 ± 133	1,417 ± 158	1,878 ± 139
Adult lesion	1,281 ± 47	1,399 ± 113	1,852 ± 205
NEHL1	1,252 ± 0	1,314 ± 0	1,791 ± 0
NEHL2	1,348 ± 0	1,440 ± 0	2,119 ± 0
Immature neuron number			
Control	498,210 ± 82,884		
Neonatal lesion	686,313 ± 85,446		
Adult lesion	364,684 ± 91,012		
NEHL1	537,482 ± 0		
NEHL2	542,677 ± 0		
$Bcl2^+$ cell number			
Control	462,736 ± 89,034		
Neonatal lesion	595,616 ± 111,930		
Adult lesion	342,397 ± 71,772		
NEHL1	545,318 ± 0		
NEHL2	617,255 ± 0		

Cell numbers and neuron soma volume in the paralaminar, lateral and basal nuclei of the amygdala in unoperated, control monkeys (n = 7), neonatal hippocampal-lesioned monkeys (n = 8), adult hippocampal-lesioned monkeys (n = 6), and nonexperimental hippocampal-lesioned monkeys (NEHL1 and NEHL2) (values ± SD).

http://doc.rero.ch